Molecular Crystals and Liquid Crystals Science and Technology. Section A. Molecular Crystals and Liquid Crystals

Publication details, including instructions for authors and subscription information:
http://www.tandfonline.com/loi/gmcl19

Optical Properties of a Switchable Diffraction Grating

Weimin Liu [a] & Jack Kelly [a]

[a] Liquid Crystal Institute and Chemical Physics Interdisciplinary Program, Kent State University, Kent, OH, 44242

Version of record first published: 24 Sep 2006

To cite this article: Weimin Liu & Jack Kelly (2001): Optical Properties of a Switchable Diffraction Grating, Molecular Crystals and Liquid Crystals Science and Technology. Section A. Molecular Crystals and Liquid Crystals, 358:1, 199-208

To link to this article: http://dx.doi.org/10.1080/10587250108028281

Mol. Cryst. and Liq. Cryst., 2001, Vol. 358, pp. 199-208
Reprints available directly from the publisher
Photocopying permitted by license only

Optical Properties of a Switchable Diffraction Grating

WEIMIN LIU and JACK KELLY

Liquid Crystal Institute and Chemical Physics Interdisciplinary Program, Kent State University, Kent, OH 44242

We have performed detailed measurements of the far field diffraction pattern of an electrically switchable liquid crystal grating. The grating, with a period of 25 microns, was formed using interdigitated aluminum electrodes with a 15 micron gap between adjacent electrodes. The homeotropically aligned liquid crystal (ZLI-4792) had a thickness of 5 microns. We measured the diffracted intensity profile of HeNe laser light (633nm) for different applied between adjacent electrodes. The amount of light diffracted into the first order relative to zeroth order is strongly dependent on the applied voltage. The locations of successive maxima and minima also shift with the applied voltage. We studied the diffraction theoretically using geometrical optics coupled with Kirchoff diffraction theory. This theoretical model is in substantial agreement with the empirical results.

Keywords: Liquid Crystals; Switchable Diffraction Grating; Geometrical Optics

1 INTRODUCTION

Diffractive properties of liquid crystal (LC) gratings have been widely investigated and found to be applicable in optical communication, optical processing and computing, diffraction optics and optical switching[1-4]. Some kinds of liquid crystal displays (LCDs) with periodic grating-like structure, such as in-plane-

switching[5,6] (IPS) and electrically-induced optical compensation[7,8] (EOC) modes behave like diffraction gratings. In these cases, we may develop practical applications by taking advantage of diffraction. However, if they are used as displays, diffraction is a shortcoming, which needs to be avoided, since it will in general lose light intensity. Therefore the understanding the diffraction characteristics of these devices will be useful either for developing the diffraction grating for potential applications or for optimizing the display performances.

Recently, we performed theoretical and experimental studies of the electro-optical response and viewing angle characteristics of the EOC mode[9]. We used the geometrical optics approach (GOA) for the optical modeling. We found that the GOA simulation was in good agreement with experiment if diffraction was taken into account and averaged out by using a Lambertian light source in the measurement.

In this paper, we present results of our studies of a quantitative investigation of the far field diffraction pattern of an electrically switchable liquid crystal grating using the same EOC cell. We performed detailed measurements of the far field diffraction pattern for different voltages applied to the LC grating. We studied the relationship between applied voltage and the amount of light diffracted into higher orders. Additionally, we studied the diffraction theoretically using GOA coupled with Kirchoff diffraction theory.

2 THEORETICAL MODEL

The structure of the LC diffraction grating used in this study is shown schematically in Fig.1, where a periodic array of interdigitated grating electrodes is on one surface of the liquid crystal (the bottom in the figure). The cell is placed between crossed polarizer and analyzer, whose transmitting axes make an angle of 45 degrees with the electrode stripes. Without an applied field, the LC director is normal to the surface everywhere (homeotropic boundary conditions). Application of a voltage to the cell induces a periodic realignment of the liquid crystal in the plane perpendicular to the electrode stripes, which we choose as the x-z plane with the z axis normal to the cell. This LC director realignment results in a periodic variation of optical path length and, in combination with the opaque aluminum electrode stripes, forms a switchable diffraction grating.

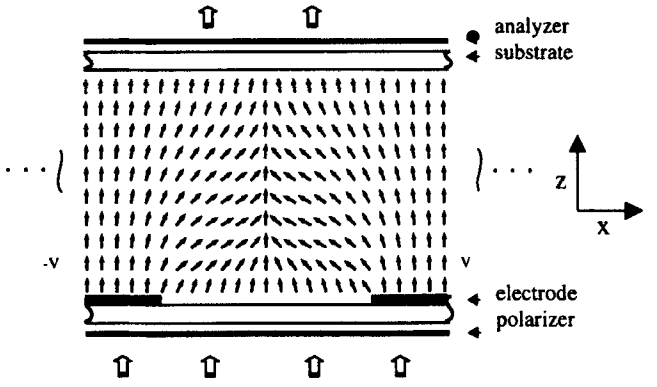

Figure 1: The structure of the switchable LC diffraction grating.

The director configuration was simulated using the Frank continuum theory. Three elastic constants were included in the calculation. Periodic boundary conditions were employed in the x-direction and infinite homeotropic surface anchoring was assumed.

The optical modeling of the grating is a combination of GOA and Kirchoff diffraction theory. With monochromatic light normally incident on the LC grating, the light propagation through the cell is claculated by GOA. Finally the diffracted light intensity is obtained from Kirchoff theory, in which the GOA optical field exiting the cell is used as the diffracting source.

We will not present the details of the GOA here[9,10]. However, we note that for normal incidence, the diffraction patterns obtained from the GOA and the Jones calculus are essentially the same for the LC grating studied here. We will show below, however, that there are some differences in transmission profile between the two approaches.

To study the diffraction, we applied the Kirchoff vector diffraction integral to the GOA field exiting the cell. When the observation point is far from the diffracting system, the diffracted field is given by:

$$\vec{E}(\vec{r}) = \frac{ie^{ik_o r}}{2\pi r}\vec{k}_o \times \int_{aperature} \hat{n} \times \vec{E}(\vec{r}\,')e^{i\vec{k}_o \cdot \vec{r}\,'} da$$

In this formula, the integral is over the region between two adjacent electrodes. $\vec{k}_0$ is the wave vector in the direction of observation, r the distance from origin to observation point, $\vec{r}'$ the coordinate of surface element da, and $\hat{n}$ the surface normal. $\vec{E}(\vec{r}')$ is the source field which is that exiting the analyzer (amplitude grating). A light source with wavelength of 633nm was employed for all of the optics calculations.

3 EXPERIMENTAL SETUP AND TEST CELL FABRICATION

In order to measure the diffraction profile from the test cell, we used the computer-controlled system shown schematically in Fig.2. Computer control and data acquisition was implemented through LabView, a Windows-based program from National Instruments. Light from a 10mW Melles Griot Helium-Neon laser (632.8nm) was directed at normal incidence to the sample cell, which was positioned with the electrode fingers oriented vertically. The diffracted light was

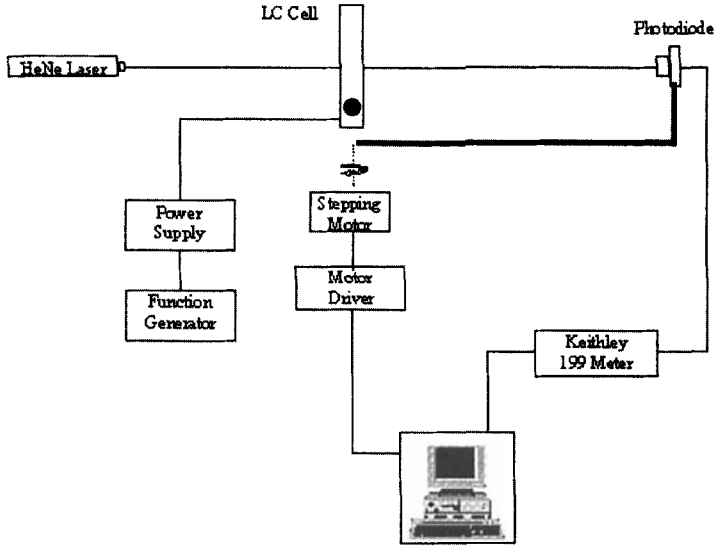

Figure 2: Experimental setup for far field diffraction pattern measurement.

detected by a photodiode fronted with a notch filter. A Keithley 199 Digital Multimeter connected to the computer via a GPIB interface monitored the photodiode signal. The photodiode was mounted on a rotatable arm with its rotation axis positioned at the cell and also vertically aligned. The rotation was performed by an Oriel stepper motor, which was controlled by computer via an RS232 port and provided an angular resolution of 0.02 degrees. The light intensity was measured as a function of the rotation angle of the photodiode with different voltages applied to the cell.

We fabricated the test cell using the same cell parameters and liquid crystal (ZLI-4792) properties as in the modeling: cell gap=5 microns, Δn=0.1, k_{11}=13.2 pN, k_{22}=6.5 pN, k_{33}=18.3 pN, $\varepsilon_{\perp}$=3.1, and $\varepsilon_{\parallel}$=8.3. The interdigitated aluminum electrodes were defined photolithographically and wet etched. The width of the etched electrodes (10 microns) and their center-to-center spacing (25 microns) was measured with a Tencor Instruments stylus profilometer. Nitto Denko 1220DU high efficiency polarizers were laminated on each side of the cell with their transmission axes oriented as described previously.

4. RESULTS AND DISCUSSION

We theoretically investigated the single slit diffraction pattern of the grating under various voltages. In general, the single slit diffraction pattern provides the envelope for the grating diffraction. Fig. 3 shows the modeling results for the diffraction pattern of a single slit for various voltages applied to the grating. Since the transmitted intensity through the cell depends on the applied voltage, each curve has been normalized by its zero order amplitude to make differences in the angular distributions more apparent. Most of the diffracted light is in the zeroth and first orders. With no applied voltage, because of the homeotropic director configuration, the liquid crystal has no effect on the grating diffraction; the normalized diffraction pattern of the grating is the typical Fraunhofer single slit pattern for a uniformly illuminated slit.

The changes is the single slit pattern result from changes in the electric field distribution exiting the liquid crystal cell. Fig. 4a shows the GOA simulation results for the light intensity exiting the analyzer

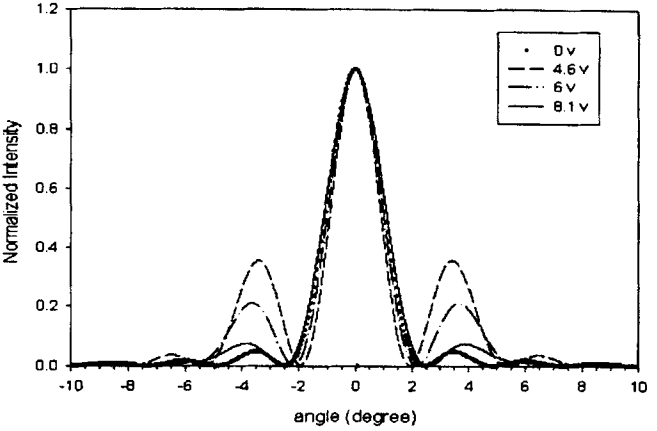

Figure 3: Calculated single slit far field diffraction patterns for the switchable grating.with different voltages applied to the electrodes.

for different applied voltages. The Jones calculus result is also shown in Fig.4b. Only at higher voltages and then only in the vicinity of the defect are there significant differences. The increased intensity near the defect in the GOA results from ray focusing which stems from the distortion of the wavefront of the extraordinary ray. It has no significant impact on the diffraction pattern. The vertical dotted lines in Fig. 4 mark the positions of the electrode edges. The portions of the curves in the electrode regions do not contribute to the diffraction integral since the light is blocked by the electrodes.

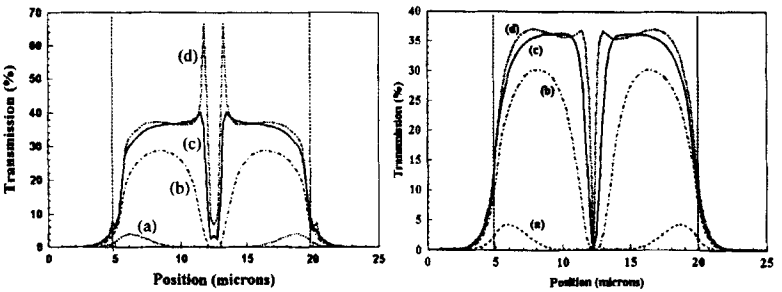

Figure 4: Calculated intensity profiles for the light exiting the grating cell: (a) GOA and (b) Jones calculus. Curves a-d in aech figure correspond to voltages of 4, 8, 12, and 16 volts, respectively.

At low voltages, there is a large region around the defect where the intensity is zero and the intensity distribution across the slit resembles that of a double slit. In this case, the single slit pattern can be viewed as arising from a double slit with a slit width given approximately by the width of one bright lobe. The envelope for this pattern should approximate a single slit with a slit width equal to the lobe width. Later we will show that this is the case.

At higher voltages, the effective birefringence of the liquid crystal staturates in the inter-electrode region and the intensity distribution becomes uniform except very near the defect. The diffraction pattern should again return to that of a uniformly illuminated single slit.

These observations gualitatively explain the voltage dependent behavior of the single slit patterns of Fig. 3. We examined the first order maximum in more detail. Fig.5 shows the strong dependence of the intensity of the first order principal maximum on applied voltage as a percentage of the zero order peak intensity. The first order diffraction maximum increases quickly from 5% at 0 volts to a maximum of 46.5% at 3.7 volts. It then decreases to about 5% again for voltages above 10 volts. For a uniformly illuminated single slit, the peak height of the first order maximum is 5% which agrees with our qualitative interpretation of the behavior above.

The location of the first order maximum also varies with the applied voltage (Fig.6). Here the behavior is somewhat more complicated than the peak height. Near 0 and 20 volts, the angle of the

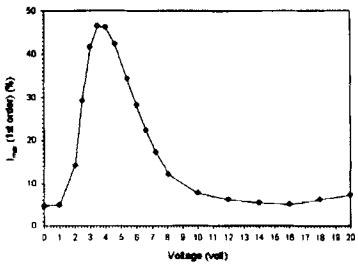

Figure 5: Variation of the single slit first order intensity with applied voltage

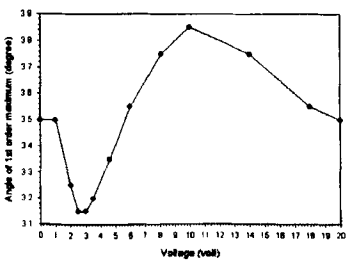

Figure 6: Position of the single slit first order maximum as a function of voltage.

maximum is near 3.5° corresponding to the location for a uniformly illuminated slit with width equal to the electrode spacing. At low voltages, where the intensity resembles a double slit, the angle of the maximum decreases. This occurs because the width of the intensity lobes increases, decreasing the inter-lobe spacing and narrowing the double slit pattern. With the crossover to single slit behavior at intermediate voltages, the angle increases to a maximum that is governed by the width of the full intensity profile. This is less than the actual slit width (See, for example, the 8 volt curve in Fig.4). Finally, with increasing voltage the effective slit width increases to the actual slit width and the angle decreases back to 3.5°.

We performed detailed measurements of the far field diffraction pattern of the switchable grating. The diffracted light intensity was measured for different voltages applied to the cell using the setup in Fig.2. Fig.7 shows the measured diffraction patterns at two voltages: 4.6 volts (Fig.7a), which is well below saturation (cf. Fig.4), and 8.1 volts (Fig.7b), which is near saturation.

In order to verify the accuracy of the model and the diffraction effects predicted by the model, we have included the model predictions in the figures as well. The number of slits we used in the model is 15. The comparison clearly demonstrates that the theoretical model is in substantial agreement with the measurement.

The calculated single slit pattern, which provides the envelope for the overall diffraction pattern, is also included in the figure. In Fig.7a we have also plotted the single slit pattern for a uniformly illuminated slit of 5 microns width, which is the approximate width of the intensity lobes at this voltage. It provides a reasonably good envelope for the single slit pattern as suggested above.

For both 4.6 volts and 8.1 volts, the positions of the intensity maxima are the same, only their amplitudes vary as a result of changes in the single slit envelope. The grating period and the wavelength of the incident light determine the positions of the intensity maxima. Because an applied voltage does not change the grating period, the positions of all maxima are the same for any voltage.

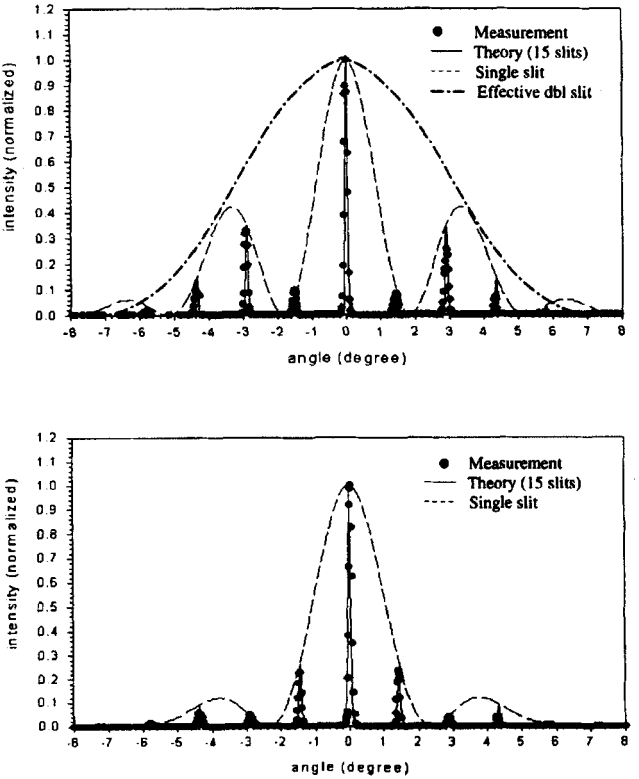

Figure 7: Measured and simulated multiple slit diffraction patterns for the switchable grating at two applied voltages: (a) 4.6 volts and (b) 8.1 volts.

5 CONCLUSION

We have investigated the optical properties of a switchable diffraction grating based on the EOC mode, both theoretically and experimentally. The theoretical predictions are in substantial agreement with experiment. This type of grating is particularly

interesting because it offers more flexibility in design because both intensity and relative peak heights can be varied simultaneously. While we presented only its application as an amplitude grating here, the EOC can also serve as a phase grating. This work is currently underway in our laboratory. We are also constructing EOC gratings with much smaller period to check the limits of our theoretical approach.

Acknowledgements

This work was supported by the NSF Science and Technology Center for Advanced Liquid Crystalline Optical Materials under grant #DMR89-20147.

References

[1] P. F. Mcmanamon, T.A. Dorschner, D.L. Corkum, L.J. Friedman, D.S. Hobbs, M. Holz, S. Liberman, H.Q. Nguyen, D.P. Pesler, R.C. Sharp, and E.A. Watson, *IEEE Proceedings, Vol.84, No.2,* 268, (1996).

[2] J. Chen, P.J. Bos, H. Vithana, and D.L. Johnson, *Appl. Phys. Lett.* **67**(18), 2588–2590 (1995).

[3] H. Murai, *Liq. Cryst.* **15**(5), 627–642 (1993).

[4] M.W. Fritch, C. Kohler, G. Hass, H. Wohler, and D.A. Mlynski, *Mol. Cryst. Liq. Cryst.,* **198,** 1–14 (1991).

[5] R. Kiefer, B. Weber, F. Windscheid, and G. Baur, *Proceedings of Japan Display'92,* 557(1992).

[6] M. Oh-e, M. Ohta, S. Aratani, K. Kondo, *Proceedings of AsiaDisplay'95,* 707(1995).

[7] S.H. Lee, H.Y. Kim, T.K. Jung, I.C. Park, Y.H. Lee, B.G. Rho, J.S. Park, and H.S. Park, *Proceedings of the 4th International Display Workshops,* Nagoya, Japan, 97(1997).

[8] K.H. Kim, S.B. Park, J. Shim, J. Chen, and J.H. Souk, *Proceedings of the 4th International Display Workshops,* Nagoya, Japan, 175(1997).

[9] W. Liu, J. Kelly, and J. Chen, *Jap. J. Appl. Phys. Vol.38* 2779–2784 (1999).

[10] J. Kelly and W. Liu, Materials Research Society 1999 Spring Meeting Book of Abstracts, D5.4, p.84.